Direct Profiling of Cancer Biomarkers in Tumor Tissue Using a Multiplexed Nanostructured Microelectrode Integrated Circuit

Zhichao Fang,[†] Leyla Soleymani,[‡] Georgios Pampalakis,[†] Maisa Yoshimoto,[§] Jeremy A. Squire,[§] Edward H. Sargent,[‡,*] and Shana O. Kelley[†,⊥,*]

[†]Department of Pharmaceutical Sciences, Leslie Dan Faculty of Pharmacy, University of Toronto, Toronto, Ontario, Canada, [‡]Department of Electrical and Computer Engineering, Faculty of Engineering, University of Toronto, Toronto, Ontario, Canada, [§]Department of Pathology and Molecular Medicine, Queen's University, Kingston, Ontario, Canada, and [⊥]Department of Biochemistry, Faculty of Medicine, University of Toronto, Toronto, Ontario, Canada

ABSTRACT The analysis of panels of nucleic acid biomarkers offers valuable diagnostic and prognostic information for cancer management. A cost-effective, highly sensitive electronic chip would offer an ideal platform for clinical biomarker readout and would have maximal utility if it was (i) multiplexed, enabling on-chip assays of multiple biomarkers, and (ii) able to perform direct (PCR-free) readout of disease-related genes. Here we report a chip onto which we integrate novel nanostructured microelectrodes and with which we directly detect cancer biomarkers in heterogeneous biological samples—both cell extracts and tumor tissues. Coarse photolithographic microfabrication defines a multiplexed sensing array; bottom-up fabrication of nanostructured microelectrodes then provides sensing elements. We analyzed a panel of mRNA samples for prostate cancer related gene fusions using the chip. We accurately identified gene fusions that correlate with aggressive prostate cancer and distinguished these from fusions associated with slower-progressing forms of the disease. The multiplexed nanostructured microelectrode integrated circuit reported herein provides direct, amplification-free, sample-to-answer in under 1 h using the 10 ng of mRNA readily available in biopsy samples.

KEYWORDS: electrochemical biosensing · nanostructures · biomarker · diagnostic · microchip

Biomarker analysis based on electronic readout has long been cited as a path to integrated, chip-based devices with cost and sensitivity appropriate for clinical testing.[1−4] The sensitivity of electronic readout is, in principle, sufficient to allow direct detection of small numbers of analyte molecules with simple instrumentation. However, despite tremendous advances in this area as well as related fields working toward new diagnostics,[1,5−17] no multiplexed chip has yet shown direct electronic detection of biomarkers in clinical samples. The challenges that have limited the implementation of such devices primarily stem from the difficulty of obtaining very low detection limits in the presence of high background levels present when complex biological samples are assayed and the challenge of generating multiplexed systems that are highly sensitive and specific.

Indeed, while nanowire, nanotube, and carbon nanotube sensors have proven useful as ultrasensitive detectors of biomolecules, they typically fall short of displaying the requisite sensitivity, specificity, and multiplexing for clinical sample analysis. For example, silicon nanowires used as field effect transistors[5,7,18] display impressive versatility in the detection of a range of analytes including nucleic acids, but low signal-to-background has limited their use with heterogeneous sample mixtures. Another elegant system relying on the use of networks of metal nanoparticles interfacing metal microleads[11] exhibits a broad dynamic range and good sequence selectivity but moderate 500 fM sensitivity and no reported performance in heterogeneous samples. Carbon nanotubes, used both as electrochemical detectors and as field effect transistors,[19,20] also suffer from low sensitivities in the picomolar range that would limit their use without enzymatic amplification. We recently reported the direct detection of a class of cancer biomarkers using electrodes based on templated gold nanowires.[21] This approach provides femtomolar sensitivity, which is sufficient for PCR-free clinical applications based on 100 ng of RNA from tumor tissue. However, the difficulty of multiplexing this platform limits its use in the profiling of multiple markers and implementation as an effective cancer diagnostic system. Clearly, more versatile and robust systems are needed to expand the range of clinical diagnostic tools available.

*Address correspondence to shana.kelley@utoronto.ca, ted.sargent@utoronto.ca.

Received for review July 3, 2009 and accepted August 30, 2009.

Published online September 8, 2009.
10.1021/nn900733d CCC: $40.75

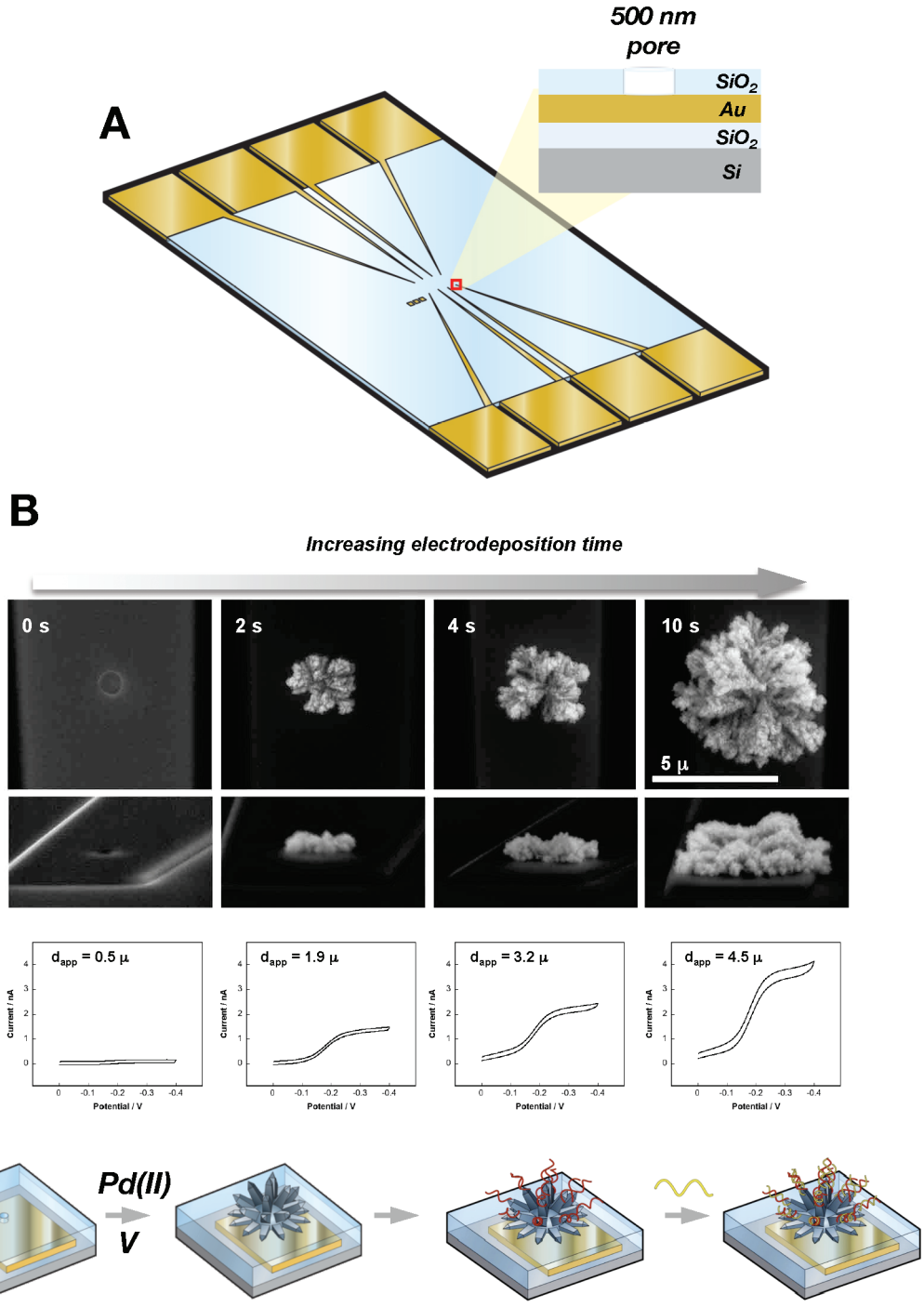

Figure 1. Fabrication of a nanostructured microelectrode (NME) chip. (A) Schematic illustration of a NME chip. A gold pattern is deposited on a silicon wafer using conventional photolithography and is then covered with a layer of SiO_2; 500 nm openings are then etched through this top layer to expose a circular section of gold. (B) Time dependence of Pd NME electrodeposition. The diameter and height of the NME as visualized with scanning electron microscopy (SEM) are controlled by manipulating deposition time. In addition, cyclic voltammograms (CVs) for 3 mM $Ru(NH_3)_6^{3+}$ demonstrate that larger electrode area is obtained with longer electrodeposition time. Approximate apparent microelectrode diameters were calculated from limiting current values. (C) Schematic illustrating steps involved in the sensing of specific sequences. NMEs are first plated in the opening using electrodeposition. Then they are modified with thiol-derivatized probe sequences, and target sequences are hybridized. The presence of the target is transduced using an electrocatalytic reporter system.

RESULTS AND DISCUSSION

We sought to generate a nanomaterial-based platform for ultrasensitive bioanalysis that is (i) highly robust and straightforward to fabricate, (ii) multiplexed and scalable, and (iii) sensitive and specific when presented with heterogeneous biological samples. To satisfy requirements (i) and (ii), we required a means of achieving reproducible placement of each individual sensing element using a scalable protocol. To address requirement (iii), we sought to incorporate nanoscale

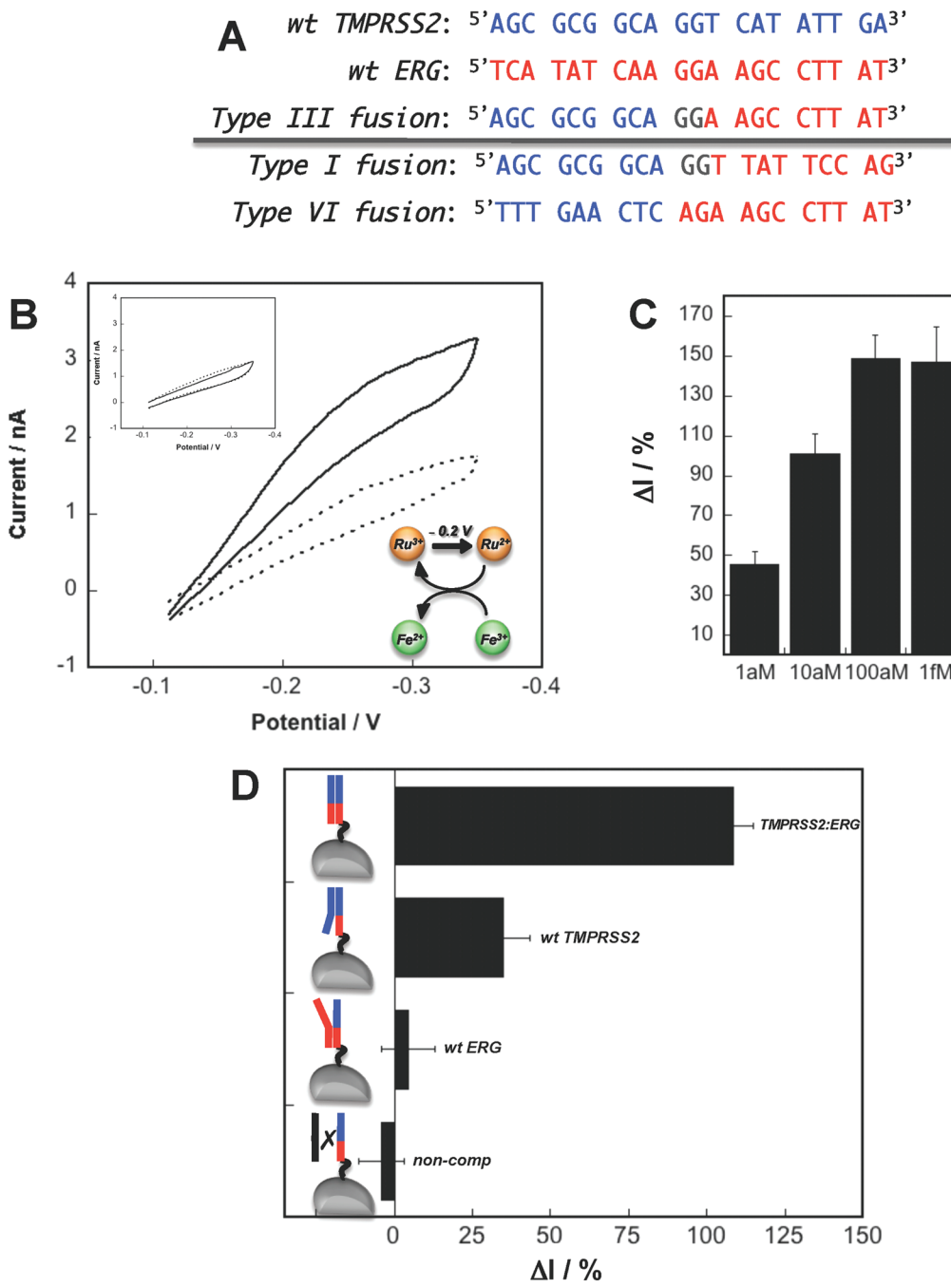

Figure 2. Ultrasensitive nucleic acid detection using a NME chip. (A) Sequences used to evaluate NMEs for nucleic acids sensing. The probe used in the studies is the complement to a portion of the type III fusion gene (seq. P1), and targets corresponded to the sequences shown for the two wild-type sequences and the fusion gene. The type I and type VI fusion sequences involve portions of the wild-type genes not shown but are listed for reference. (B) Cyclic voltammograms illustrating electrocatalytic signals before (dotted line) and after (solid line) hybridization with 100 fM cDNA target. The inset shows the response of a sensor modified with the same probe to the same concentration of a noncomplementary sequence. (C) Concentration dependence of NME sensor response. Average Δ*I* values represent averages of over five trials, and standard error of trials is shown. (D) Differentiation of related sequences: a fully complementary target (T1) corresponding to the type III gene fusion, half-complementary targets (T2 and T3) corresponding to the wild-type TMPRSS2 and ERG genes, and noncomplementary target (T4); 100 fM of DNA targets in 25 mM sodium phosphate (pH 7) and 25 mM NaCl was incubated at the PNA-modified NMEs at 37 °C for 60 min.

features into our sensing array. Prior work has illustrated the advantages of nanostructures for biomolecular sensing,[6,22] consistent with the idea that the capture of biomolecular analytes can be rendered inefficient when probe monolayers are immobilized on bulk surfaces. The production of arrayed nanostructured sensing elements, however, can be labor-intensive and prone to low reproducibility. Electron-beam lithography provides the needed control over nanoscale features and their placement; however, it is

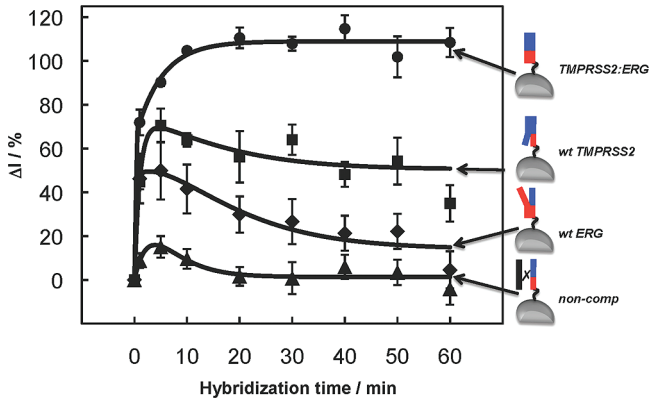

Figure 3. Kinetics of DNA hybridization at NMEs. Ru(III)/Fe(III) electrocatalysis was used to monitor signal changes when PNA-modified NMEs were incubated with 100 fM of DNA targets with different complementarities. The hybridization signal for fully complementary targets continued to increase until reaching a plateau after 20 min, while other targets with partial or no complementarity showed large initial signals with attenuation of the signal over time. Hybridization performed under the same conditions as those described in Figure 2. Data fits are shown to illustrate general behavior of the time dependence and do not represent a specific kinetic model.

a serial technique not presently suited to low-cost, high-volume chip production.

Our approach was instead to use cost-effective conventional photolithography to position and address our electrodes and then find a means to bring about, with a high degree of reproducibility, the nanostructuring of these microelectrodes. Figure 1A shows our 8-fold multiplexed chip. A 350 nm thick gold layer was patterned on a silicon chip to create eight 5 μm wide Au wires attached to large metal pads that would serve as external contacts. SiO_2 was then deposited as a passivating layer and patterned to create apertures with 500 nm diameters at the end of each of the Au wires. These openings were created to serve as individual templates for controlled, local growth of nanostructures. We then used palladium electrodeposition to deposit metal in the patterned apertures (Figure 1B). We found that we were able to regulate the size of the nanostructures by varying the deposition time. We were readily able to confine the diameter of the structures to the ultramicroelectrode regime (<10 u). Under conditions enabling rapid metal deposition, the surfaces of the microelectrodes displayed a high level of nanostructuring, with feature sizes of approximately 20 nm. This type of fine nanostructuring is proposed to promote hybridization by facilitating display of probe sequences on nanostructures with dimensions that approach those of biomolecules.[23] These metal structures displayed ideal microelectrode behavior, exhibiting low capacitive currents and high steady-state plateau currents (Figure 1B).

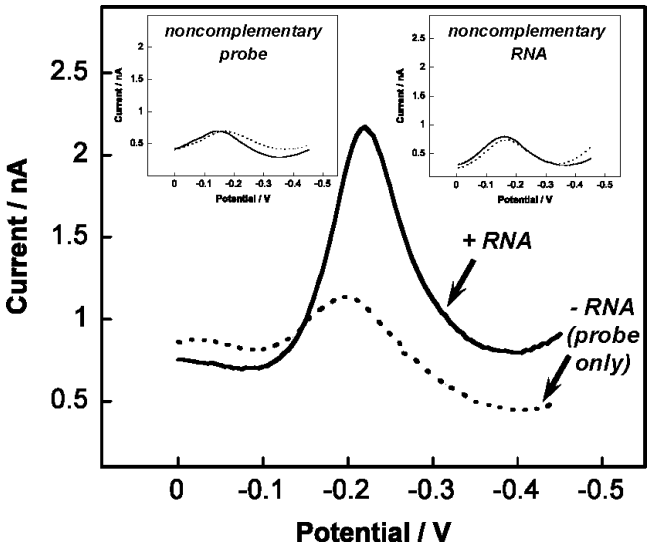

Figure 4. Detection of a prostate-cancer-associated gene fusion in VCaP RNA. RNA (10 ng) from VCaP (fusion positive) or DU145 cells (fusion negative) was incubated with PNA probe-modified NMEs for 60 min at 37 °C. The VCaP RNA, when matched with an NME bearing a probe complementary to the type III gene fusion (seq. P1), produced a large change in signal (center plot), while if a type I probe (seq. P2) was used instead, no change in signal was observed (left inset). The DU145 RNA also did not produce an appreciable change in the electronic signal when incubated with a type III probe (right inset). These controls verify that the hybridization observed with VCaP RNA and the type III probe is specific.

In order to make these nanostructured microelectrodes (NMEs) functional as nucleic acids biosensors, we modified them with thiolated peptide−nucleic acid (PNA) probes (Figure 1C). The use of PNA as a probe molecule has been shown previously to increase the sensitivity of biosensing assays[24,25] and is particularly advantageous in electrochemical assays because it produces lowered background currents. To transduce nucleic acid hybridization into an electrical signal, we employed an electrocatalytic reporter system previously developed by our laboratory.[26] This reporter system relies on the accumulation of $Ru(NH_3)_6^{3+}$ at electrode surfaces when polyanionic species such as nucleic acids bind and the catalysis of the reduction of Ru(III) *via* the inclusion of $Fe(CN)_6^{3-}$, which regenerates Ru(III) and allows multiple reductions per metal center. When PNA-modified NMEs were challenged with a complementary sequence, detectable signal changes could be clearly detected through the femtomolar concentration range (Figure 2). Negligible signal changes were observed with completely noncomplementary sequences.

The cancer biomarkers selected for analysis on this platform are a group of gene fusions specific to prostate cancer (Figure 2A). These fusions, resulting from a chromosomal translocation that joins the ERG and TMPRSS2 genes, were recently discovered and appear in at least 50% of prostate tumors.[27,28] Furthermore, there are ~20 sequence types that feature different fusion sites, and the exact type of fusion present in a tumor appears to correlate with its aggressiveness and metastatic potential.[29] These sequences are therefore not only promising diagnostic markers but also factors with prognostic value.

The discrimination of gene fusion sequences from the half-complementary wild-type sequences was investigated with NME sensors modified with a probe

complementary to the splice site of the most common type III fusion challenged with (1) the fusion target (seq. T1), (2) the sequence corresponding to the wild-type TMPRSS2 gene (seq. T2), and (3) a sequence corresponding to the wild-type ERG gene (seq. T3) (Figure 2A,D). A completely noncomplementary control was also assayed (seq. T4). With a hybridization time of 60 min, large signal increases were observed with the fully complementary target, while a much lower signal change was seen with the TMPRSS2 target. The ERG target produced an even lower signal change, and that observed with the noncomplementary sequence was negligible. The TMPRSS2 target binds to the portion of the probe located at the end of the sequence not attached to the electrode, while the ERG target binds to the portion of the probe located at the end tethered to the electrode surface. The different signal levels observed may indicate that the most accessible side of the probe is better able to bind incoming target molecules, while hybridization with the more buried part of the sequence is inefficient. In addition, the fact that the noncomplementary portion of T2 has higher homology to the probe may also influence the higher background level. A recent study conducted using this same platform showed that it possesses the ability to discriminate sequences that differ by only a single nucleotide,[30] verifying that the selectivity of the sensors is high, but the length of the sequences under study here may make it difficult to completely eliminate cross hybridization.

To determine whether the hybridization of the different targets required the full 60 min time period originally tested for accurate readout, the electrocatalytic signals were monitored at a variety of intervals within the window originally tested (Figure 3). Interestingly, the rise of the signals is very fast, with significant current changes observed within 2 min. Over the total 60 min period, however, the signals for the half-complementary and noncomplementary sequences fall noticeably, with 20−50% of the 2 min signal vanishing by 60 min. It appears that, for sequences that are not fully complementary, some nonspecific binding occurs in the first few minutes of exposure of the NME sensor to the target solution, but these complexes do not remain stable and do not remain immobilized on the electrode. Thus, while noncomplementary sequences can be discriminated from complementary sequences with short hybridization times, longer times increase the differential signal changes and thus the degree of specificity.

The performance of these nanostructured microelectrodes as nucleic acid detectors indicated that the patterned structures were indeed sensitive and specific when used under appropriate hybridization conditions. We therefore sought to prove that multiplexed chip-based NMEs could be used to assay cancer biomarkers presented in heterogeneous biological samples.

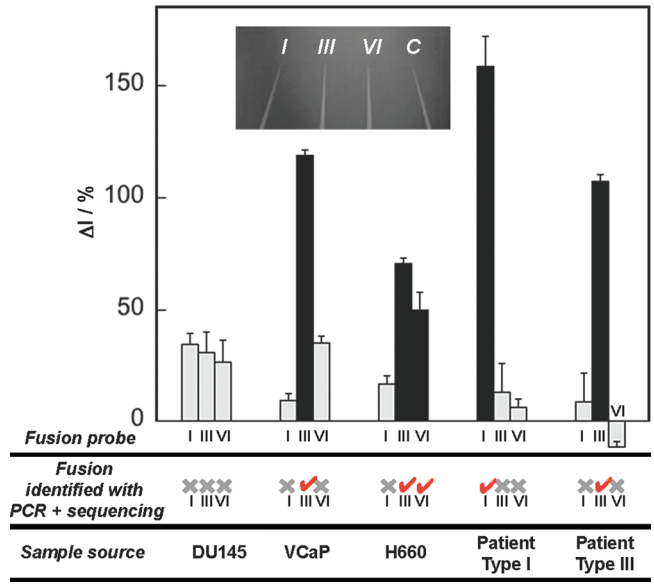

Figure 5. Multiplexed profiling of prostate-cancer-related gene fusions in clinical samples and cell lines. Patient samples and three cell lines were analyzed for three different types of prostate-cancer-related gene fusions: type I, type III, and type VI. Ten nanograms of mRNA isolated from two tumor samples was tested, one that was positive for the type I fusion, and one that was positive for the type III fusion. In addition, three cell lines were tested: VCaP (type III positive), NCI-H660 (type III and VI positive), and DU145 (fusion negative). Probes corresponding to the splice sites of each fusion sequence (seq. P1, P2, and P3) were immobilized on separate NMEs on a chip, along with a control (C), and electrocatalytic signals were collected after 60 min hybridization with RNA samples. The RNA solutions had a concentration of 1 ng/μL. Sequences that were also observed after PCR and direct sequencing are highlighted as black bars. The inset depicts an image of the multiplexed chip used for the analysis, which had a type I, type III, type VI, and control (C) probe immobilized on separate leads.

To explore this capability, cell extracts and tumor samples from prostate cancer patients were assessed to determine whether the sensitivity and specificity of the system was robust enough for clinical testing. We first analyzed mRNA isolated from two prostate cancer cell lines: VCaP and DU145 (Figure 4). The former cell line is type III fusion positive, and the latter is fusion negative.[28] No appreciable signal changes occurred when 10 ng of mRNA from the cell line that lacks this sequence was incubated with a NME displaying a probe complementary to the type III fusion (seq. P1), while large signal increases were observed in the presence of 10 ng of mRNA from the cell line that does contain the type III fusion. In addition, the modification of NMEs with a probe complementary to a different fusion (seq. P2) did not yield a significant signal with positive mRNA sample. The detection of the fused gene is therefore highly specific. These results are significant, as efficiency in the use of sample (10 ng) and the total time required for analysis (less than 1.5 h) significantly improve upon other detection methods such as fluorescence *in situ* hybridization (FISH) and sequencing.

The ultimate application of the NME chip is the direct, multiplexed analysis of a panel of cancer biomarkers in relevant patient samples. To test the perfor-

mance of our device for this type of application, we analyzed a panel of mRNA samples collected from cell lines and clinical tumor samples for a series of gene fusions (Figure 5). We obtained a group of samples that would allow the detection of the three most common types of prostate cancer gene fusions: type I, type III, and type VI. Different clinical outcomes are associated with these sequences, with type III fusions being the most common but correlating with low cancer recurrence rates, whereas type I and VI fusions are correlated with aggressive cancers with high levels of recurrence.[29] It is therefore of great interest to be able to differentiate these fusions in tumors, and a method that would permit their presence or absence to be assessed quickly and straightforwardly would be of value in their further study and validation as diagnostic biomarkers.

Probes complementary to each of the three fusions were deposited on their respective electrodes on NME chips, and five different mRNA samples were profiled for the presence of different gene fusions in a multiplexed format (Figure 5). Three cell lines were tested: VCap (type III positive),[28] NCI-H660 (type III and VI positive),[31] and DU145 (fusion negative).[28] In addition, two tumor samples (tissues collected by radical prostatectomies) were tested, one that was positive for the type I fusion, and one that was positive for the type III fusion, as confirmed by conventional sequencing. In each case, all experiments took less than 2 h and required only 10 ng of mRNA. By analyzing the electrochemical signals collected at NMEs displaying different probes, we ascertained, as seen in Figure 5, the identity of fused genes present in each sample. For example, in the patient sample containing the type I fusion (as verified by sequencing), the current values observed at each probe-modified NME decreased in the following order: I $\gg$ III $>$ VI. In the patient sample containing the type III fusion, the electronic signals again pointed to the correct identity of the fusion with probe III $\gg$ I $>$ VI. These results, and those obtained with DU145, VCaP, and H660 cellular RNA, where electronic profiling correctly called the absence or presence of gene fusions, indicate that NME chips are able to profile these important biomarkers in complex samples and to distinguish biomarker profiles associated with different clinical outcomes.

The detection platform described here is not only specific, sensitive, and robust, but it is also practical and scalable. The reproducible fabrication method we chose is amenable to the production of probe-modified chips using the same photolithographic technologies in widespread use in consumer electronics microchip fabrication, and only simple, inexpensive instrumentation is needed for readout. Microfluidics are not required for automated analysis, as hybridization can be performed and read out in a single reaction vessel, as shown in Figure 3. This system represents an attractive alternative to PCR-based methods that are sensitive but difficult to automate in a clinical setting.

In sum, the new multiplexed electrode platform we describe here is the first to read directly a panel of cancer biomarkers in clinically relevant samples using electronic signals. The array enabling these measurements features microelectrodes that possess controllable and versatile nanotexturing essential for sensitivity. The system combines these nanotextured electrodes with rapid catalytic readout to achieve a long-standing goal: the multiplexed analysis of cancer biomarkers using an inexpensive and practical platform.

METHODS

Chip Fabrication. Chips were fabricated at the Canadian Photonics Fabrication Center. Three inch silicon wafers were passivated using a thick layer of thermally grown silicon dioxide. A 350 nm gold layer was deposited on the chip using electron-beam-assisted gold evaporation. The gold film was patterned using standard photolithography and a lift-off process. A 500 nm layer of insulating silicon dioxide was deposited using chemical vapor deposition; 500 nm apertures were imprinted on the electrodes using standard photolithography, and 2 mm $\times$ 2 mm bond pads were exposed using standard photolithography.

Fabrication of Nanostructured Microelectrodes. Chips were cleaned by rinsing in acetone, IPA, and DI water for 30 s and dried with a flow of nitrogen. All electrodeposition was performed at room temperature with a Bioanalytical Systems Epsilon potentiostat with a three-electrode system featuring a Ag/AgCl reference electrode and a platinum wire auxiliary electrode; 500 nm apertures on the fabricated electrodes were used as the working electrode and were contacted using the exposed bond pads. Palladium NMEs were fabricated in a palladium bath containing 5 mM solution of H_2PdCl_4 and 0.5 M $HClO_4$ at -250 mV for 10 s using DC potential amperometry.

Preparation and Purification of Oligonucleotides. All synthetic oligonucleotides were stringently purified by reversed-phase HPLC. The following probe and target sequences were used in experiments. Seq. P1, type III fusion probe (PNA): NH_2-Cys-Gly-ATA AGG CTT CCT GCC GCG CT-$CONH_2$. Seq. P2, type I fusion probe (PNA): NH_2-Cys-Gly-CTG GAA TAA CCT GCC GCG CT-$CONH_2$. Seq. P3, type VI fusion probe (PNA): NH_2-Cys-Gly-ATA AGG CTT CTG AGT TCA AA-$CONH_2$. Seq. T1 (type III TMPRSS2:ERG fusion DNA target): 5′-AGC GCG GCA GGA AGC CTT AT-3′. Seq. T2 (WT TMPRSS2 DNA target): 5′-AGC GCG GCA GGT CAT ATT GA-3′. Seq. T3 (WT ERG DNA target): 5′-TCA TAT CAA GGA AGC CTT AT-3′. Seq. T4 (noncomlementary DNA target): 5′-TTT TTT TTT TTT TTT TTT TT-3′. Oligonucleotides were quantitated by measuring absorbance at 260 nm and ext coefficients calculated using http://www.idtdna.com/analyzer/Applications/OligoAnalyzer/.

Modification of NMEs with PNA Probes. A solution containing 500 nM thiolated single-stranded PNA, 25 mM sodium phosphate (pH 7), and 25 mM sodium chloride was heated at 50 °C for 10 min. A suitable amount of 10 mM MCH was then added to make the final MCH concentration of 100 nM; 0.5−10 μL (depending on the degree of multiplexing) of this mixture was deposited on the NMEs in a dark humidity chamber overnight at 4 °C. The NMEs were rinsed in 25 mM sodium phosphate (pH 7) and 25 mM NaCl buffer before measurements.

Electrochemical Measurements. Electrochemical signals were measured in solutions containing 10 μM $Ru(NH_3)_6^{3+}$, 25 mM sodium phosphate (pH 7), 25 mM sodium chloride, and 4 mM $Fe(CN)_6^{3-}$. Differential pulse voltammetry (DPV) signals before and after hybridization were measured using a potential step of 5 mV, pulse amplitude of 50 mV, pulse width of 50 ms, and a

pulse period of 100 ms. Cyclic voltammetry signals before and after hybridization were collected with a scan rate of 100 mV/s. Limiting reductive current (I) was quantified by subtracting the background at 0 mV from the cathodic current at −300 mV in a cyclic voltammetry signal. Signal changes corresponding to hybridization were calculated as follows: $\Delta I = (I_{ds} - I_{ss})/I_{ss} \times 100\%$ (ss = before hybridization, ds = after hybridization).

Hybridization Protocol. Hybridization solutions typically contained target sequences in 25 mM sodium phosphate (pH 7) and 25 mM NaCl. Electrodes were incubated at 37 °C in a humidity chamber in the dark for 60 min and were washed extensively with buffer before electrochemical analysis.

Isolation of mRNA. The mRNAs were extracted from cell lines and patient tissue samples with the Dynabeads mRNA Direct Kit (Invitrogen). Two typical prostate cancer tissue samples were obtained from radical prostatectomies collected by from the Cooperative Human Tissue Network. The tissue was stored at −85 °C until tumor-rich tissue was selected for mRNA extraction. The concentrations of mRNA targets were measured by NanoDrop ND-1000 of Thermo Fisher Scientific (USA). All of the fusion sequences were confirmed by RT-PCR and direct sequencing.

Kinetic Measurements of DNA Hybridization at NMEs. PNA (seq. 2)-modified NMEs were prepared as described above. Rinsed NMEs were immersed in a solution containing 10 μM $Ru(NH_3)_6^{3+}$, 4 mM $Fe(CN)_6^{3-}$, 100 fM DNA target (seq. 4−7), 25 mM sodium phosphate (pH 7), and 25 mM NaCl. The electrocatalytic CV signals were obtained as described above. All measurements were performed at 37 °C.

Acknowledgment. The authors wish to acknowledge Genome Canada (E.H.S. and S.O.K.), the Ontario Ministry of Research and Innovation (S.O.K.), the Prostate Cancer Research Foundation (S.O.K.), the Ontario Centres of Excellence (S.O.K.), NSERC (S.O.K.), the Ontario Institute of Cancer Research (S.O.K. and E.H.S.), the Canada Foundation for Innovation (S.O.K.), and the Cancer Research Society (J.S. and M.Y.) for financial support of this work. We also thank Stuart Rae for preparation of the RNA samples from cell lines and tissue.

REFERENCES AND NOTES

1. Bell, J. Predicting Disease Using Genomics. *Nature* **2004**, *429*, 453–456.
2. Ludwig, J. A.; Weinstein, J. N. Biomarkers in Cancer Staging, Prognosis and Treatment Selection. *Nat. Rev. Cancer* **2005**, *5*, 845–856.
3. Drummond, T. G.; Hill, M. G.; Barton, J. K. Electrochemical DNA Sensors. *Nat. Biotechnol.* **2003**, *21*, 1192–1199.
4. Weston, A. D.; Hood, L. Systems Biology, Proteomics, and the Future of Health Care: Toward Predictive, Preventative, and Personalized Medicine. *J. Proteome Res.* **2004**, *3*, 179–196.
5. Cui, Y.; Wei, Q.; Park, H.; Lieber, C. M. Nanowire Nanosensors for Highly Sensitive and Selective Detection of Biological and Chemical Species. *Science* **2001**, *293*, 1289–1292.
6. Gasparac, R.; Taft, B. J.; Lapierre-Devlin, M. A.; Lazareck, A. D.; Xu, J. M.; Kelley, S. O. Ultrasensitive Electrocatalytic DNA Detection at Two- and Three-Dimensional Nanoelectrodes. *J. Am. Chem. Soc.* **2004**, *126*, 12270–12271.
7. Hahm, J.; Lieber, C. M. Direct Ultrasensitive Electrical Detection of DNA and DNA Sequence Variations Using Nanowire Nanosensors. *Nano Lett.* **2004**, *4*, 51–54.
8. Katz, E.; Willner, I. Probing Biomolecular Interactions at Conductive and Semiconductive Surfaces by Impedance Spectroscopy: Routes to Impedimetric Immunosensors, DNA-Sensors, and Enzyme Biosensors. *Electroanalysis* **2003**, *15*, 913–947.
9. Munge, B.; Liu, G. D.; Collins, G.; Wang, J. Multiple Enzyme Layers on Carbon Nanotubes for Electrochemical Detection Down to 80 DNA Copies. *Anal. Chem.* **2005**, *77*, 4662–4666.
10. Nicewarner-Pena, S. R.; Freeman, R. G.; Reiss, B. D.; He, L.; Pena, D. J.; Walton, I. D.; Cromer, R.; Keating, C. D.; Natan, M. J. Submicrometer Metallic Barcodes. *Science* **2001**, *294*, 137–141.
11. Park, S. J.; Taton, T. A.; Mirkin, C. A. Array-Based Electrical Detection of DNA with Nanoparticle Probes. *Science* **2002**, *295*, 1503–1506.
12. Steemers, F. J.; Ferguson, J. A.; Walt, D. R. Screening Unlabeled DNA Targets with Randomly Ordered Fiber-Optic Gene Arrays. *Nat. Biotechnol.* **2000**, *18*, 91–94.
13. Vlassiouk, I.; Kozel, T.; Siwy, Z. Biosensing with Nanofluidic Diodes. *J. Am. Chem. Soc.* **2009**, *131*, 8211–8220.
14. Xiao, Y.; Qu, X. G.; Plaxco, K. W.; Heeger, A. J. Label-Free Electrochemical Detection of DNA in Blood Serum *via* Target-Induced Resolution of an Electrode-Bound DNA Pseudoknot. *J. Am. Chem. Soc.* **2007**, *129*, 11896–11897.
15. Yi, M. Q.; Jeong, K. H.; Lee, L. P. Theoretical and Experimental Study towards a Nanogap Dielectric Biosensor. *Biosens. Bioelectron.* **2005**, *20*, 1320–1326.
16. Zhang, Y. C.; Pothukuchy, A.; Shin, W.; Kim, Y.; Heller, A. Detection of Similar to 10^3 Copies of DNA by an Electrochemical Enzyme-Amplified Sandwich Assay with Ambient O_2 as the Substrate. *Anal. Chem.* **2004**, *76*, 4093–4097.
17. Zheng, G.; Patolsky, F.; Cui, Y.; Wang, W. U.; Lieber, C. M. Multiplexed Electrical Detection of Cancer Markers with Nanowire Sensor Arrays. *Nat. Biotechnol.* **2005**, *23*, 1294–1301.
18. Gao, Z.; Agarwal, A.; Trigg, A. D.; Singh, N.; Fang, C.; Tung, C. H.; Fan, Y.; Buddharaju, K. D.; Kong, J. Silicon Nanowire Arrays for Label-Free Detection of DNA. *Anal. Chem.* **2007**, *79*, 3291–3297.
19. Li, J.; Ng, H. T.; Cassell, A.; Fan, W.; Chen, H.; Ye, Q.; Koehne, J.; Han, J.; Meyyappan, M. Carbon Nanotube Nanoelectrode Array for Ultrasensitive DNA Detection. *Nano Lett.* **2003**, *3*, 597–602.
20. Star, A.; Tu, E.; Niemann, J.; Gabriel, J. C. P.; Joiner, C. S.; Valcke, C. Label-Free Detection of DNA Hybridization Using Carbon Nanotube Network Field-Effect Transistors. *Proc. Natl. Acad. Sci. U.S.A.* **2006**, *103*, 921–926.
21. Fang, Z.; Kelley, S. O. Direct Electrocatalytic mRNA Detection Using PNA-Nanowire Sensors. *Anal. Chem.* **2009**, *81*, 612–617.
22. Lapierre-Devlin, M. A.; Asher, C. L.; Taft, B. J.; Gasparac, R.; Roberts, M. A.; Kelley, S. O. Amplified Electrocatalysis at DNA-Modified Nanowires. *Nano Lett.* **2005**, *5*, 1051–1055.
23. Soleymani, L.; Fang, Z.; Sargent, E. H.; Kelley, S. O. Programming the Sensitivity of Nucleic Acids Detction using Controlled Nanostructuring. *Nat. Nanotechnol.* In press. DOI: 10.1038/nnano.2009.276.
24. Kerman, K.; Saito, M.; Tamiya, E. Electroactive Chitosan Nanoparticles for the Detection of Single-Nucleotide Polymorphisms Using Peptide Nucleic Acids. *Anal. Bioanal. Chem.* **2008**, *391*, 2759–2767.
25. Liu, J.; Tiefenauer, L.; Tian, S.; Nielsen, P. E.; Knoll, W. PNA−DNA Hybridization Study Using Labeled Streptavidin by Voltammetry and Surface Plasmon Fluorescence Spectroscopy. *Anal. Chem.* **2006**, *78*, 470–476.
26. Lapierre, M. A.; O'Keefe, M.; Taft, B. J.; Kelley, S. O. Electrocatalytic Detection of Pathogenic DNA Sequences and Antibiotic Resistance Markers. *Anal. Chem.* **2003**, *75*, 6327–6333.
27. Kumar-Sinha, C.; Tomlins, S. A.; Chinnaiyan, A. M. Recurrent Gene Fusions in Prostate Cancer. *Nat. Rev. Cancer* **2008**, *8*, 497–511.
28. Tomlins, S. A.; *et al.* Recurrent Fusion of TMPRSS2 and ETS Transcription Factor Genes in Prostate Cancer. *Science* **2005**, *310*, 644–648.
29. Wang, J.; Cai, Y.; Ren, C.; Ittmann, M. Expression of Variant TMPRSS2/ERG Fusion Messenger RNAs is Associated with Aggressive Prostate Cancer. *Cancer Res.* **2006**, *66*, 8347–8351.
30. Yang, H.; Hui, A.; Soleymani, L.; Pampalakis, G.; Liu, F. F.; Sargent, E. H.; Kelley, S. O. Direct, Electronic MicroRNA Detection Reveals Differential Expression Profiles in 30 Minutes. *Angew. Chem., Int. Ed.* In press.
31. Mertz, K. D.; *et al.* Molecular Characterization of TMPRSS2-ERG Gene Fusion in the NCI-H660 Prostate Cancer Cell Line: A New Perspective for an Old Model. *Neoplasia* **2007**, *9*, 200–206.